Eur. Phys. J. D **34**, 165–168 (2005)
DOI: 10.1140/epjd/e2005-00138-1

THE EUROPEAN PHYSICAL JOURNAL D

Tuning the surface plasmon resonance by preparation of gold-core/silver-shell and alloy nanoparticles

F. Hubenthal[a], T. Ziegler, C. Hendrich, M. Alschinger, and F. Träger

Institut für Physik and Center for Interdisciplinary Nanostructure Science and Technology — CINSaT, Universität Kassel, Heinrich-Plett-Str. 40, 34132 Kassel, Germany

Received 6 September 2004
Published online 13 July 2005 –

Abstract. For many applications like surface enhanced Raman scattering or fluorescence microscopy in which the optical field enhancement associated with surface plasmon excitation is exploited, tunability of this collective resonance over a wide energy range is required. For this purpose we have investigated Au/Ag alloyed and Au-core/Ag-shell nanoparticles with different shell thicknesses. The core-shell nanoparticles were prepared by subsequent deposition of Au and Ag atoms on quartz substrates followed by diffusion and nucleation. The surface plasmon frequency could be stabilized at 2.2 eV independent of the Ag-shell thickness. Annealing of the core-shell nanoparticles makes possible tuning of the resonance frequency from 2.2 eV ($\lambda = 564$ nm) to 2.6 eV ($\lambda = 477$ nm). Theoretical modelling allows us to attribute this observation to the formation of alloy nanoparticles.

PACS. 71.45.Gm Exchange, correlation, dielectric and magnetic response functions, plasmons – 61.46.+w Nanoscale materials: clusters, nanoparticles, nanotubes, and nanocrystals

1 Introduction

The optical properties of noble and alkali metal nanoparticles are dominated by so-called surface plasmon resonances or more precisely, by surface plasmon polariton excitations. Contrary to bulk materials plasmon polaritons can be excited in nanoparticles by electromagnetic radiation, hence distinct resonances in the optical spectra are observed. Associated with the surface plasmon resonance is a field enhancement in the vicinity of the particles surface, which is of special interest, because it is exploited in surface enhanced Raman spectroscopy [1–3], surface enhanced fluorescence [4–6] and confocal microscopy [7], and in all-optical switching devices [8] or waveguides [9, 10]. For optimum interaction of the nanoparticles with a given wavelength, certain tailor-made sizes and/or shapes are needed. However, this may not guarantee highest field enhancement factors if pure gold or silver nanoparticles are used. In order to optimize the absorption wavelength, the amplitude and the enhancement factor independently, we have prepared and investigated Au-core/Ag-shell and Au/Ag alloy nanoparticles.

2 Experimental

The nanoparticles were prepared under ultra high vacuum conditions (base pressure $<10^{-8}$ mbar) by deposition of gold and silver atoms on quartz substrates (Crystec, orientation (0001)), followed by diffusion and nucleation, i.e. Volmer-Weber-growth. The flux of the atoms was monitored with a quartz crystal microbalance (Infincon, 6 MHz, 008-010-G10) and set to 8×10^{14} atoms/cm^2 min. For the nanoparticles examined here, we have first deposited 1.4×10^{16} Au atoms/cm^2 on quartz substrates. After the growth of gold nanoparticles different amounts of silver atoms were adsorbed. As a result of the growth process nanoparticle ensembles that exhibit size and shape distributions with widths of about 30% and 40% are produced [11,12]. This leads to an inhomogeneously broadened surface plasmon resonance.

Due to the growth process, large nanoparticles have a pronounced oblate shape. Therefore, one can excite two plasmon modes in the nanoparticles if p-polarized light is used, as depicted in Figure 1. A high energetic (1,0)-mode that corresponds to electron excitations along the short axis and a low energetic (1,1)-mode in the direction of the long axis [13]. The nanoparticles are characterized by two parameters, (i) the axial ratio a/b, where a denotes the short axis and b the long axis of the oblate nanoparticles and (ii) the equivalent radius R_{eq}, which is the radius of a sphere with the same volume as the actual particle. For nanoparticles with R_{eq} in the range between 1 nm and 20 nm the position of the surface plasmon resonance depends mainly on the shape, i.e. the axial ratio [13]. If the axial ratio a/b drops off, the (1,0)-mode shifts to higher energy and the (1,1)-mode to lower energy (see Fig. 1).

[a] e-mail: hubentha@physik.uni-kassel.de

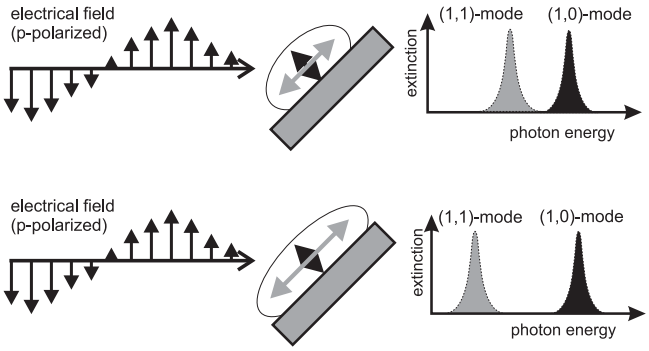

Fig. 1. The surface plasmon resonance splits into two modes due to the oblate shape of the nanoparticles. The position of these modes depend mainly on the axial ratio, since for small nanoparticles with radii between 1 nm and 20 nm the (1,1)-mode shifts to lower and the (1,0)-mode to higher energies, if the axial ratio shrinks. If *s*-polarized light is used instead of *p*-polarized light only the (1,1)-mode can be excited. Note that the figure is not drawn to scale.

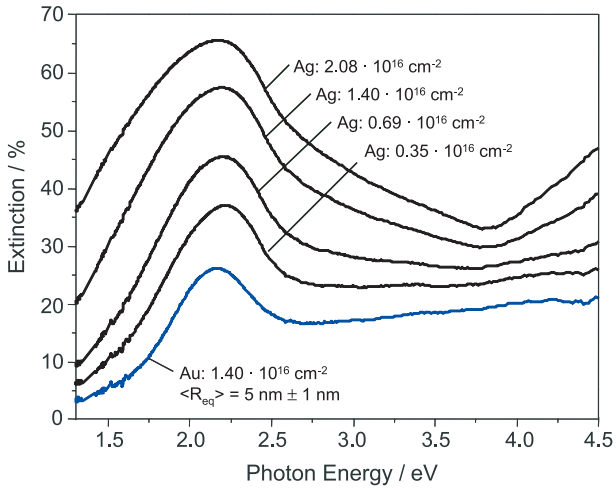

Fig. 2. Extinction spectra of pure gold and core-shell nanoparticles with different coverages of silver, measured with *s*-polarized light. After the deposition of 2.08×10^{16} atoms/cm^2 the core-shell nanoparticles consist of 40% Au and 60% Ag.

All optical spectra were recorded with a Xe-arc lamp (Osram, XBO 450W/1) in combination with a monochromator (Amko, 600 lines/mm, blaze: 400 nm). The angle of incidence was set to 45°. To exclude any influence of the (1,0)-mode on the measurements *s*-polarized light was used. Therefore, the (1,0)-mode can not be excited and only the (1,1)-mode appears in the spectra. The samples were further characterized by scanning force microscopy in order to extract the mean equivalent radii from the number density of the nanoparticles. The mean axial ratios of the entire nanoparticle ensembles were determined by theoretical modelling of the extinction spectra using the quasistatic approximation [13], which holds for the investigated nanoparticles with $R_{eq} \ll \lambda$.

3 Results and discussion

In the first step, 1.4×10^{16} gold atoms/cm^2 was evaporated on a quartz substrate. Nanoparticles with a plasmon resonance at 2.15 eV (Fig. 2), corresponding to an average axial ratio of $\langle a/b \rangle = 0.23$ (calculated with the quasistatic approximation) were generated. The average equivalent radius of the pure gold-nanoparticles was determined to be $\langle R_{eq} \rangle = 5 \pm 1$ nm. Subsequently, silver was deposited with increasing coverages, varying from 0.35×10^{16} atoms/cm^2 to 2.08×10^{16} atoms/cm^2 onto the substrate covered already with the gold nanoparticles. A monotonous increase of the extinction signal from 25% to 65% due to the higher amount of material was observed. Interestingly only a slight blue-shift of the plasmon resonance frequency to 2.2 eV was seen although the nanoparticles are supposed to get more oblate during growth, i.e. a red-shift of the plasmon resonance is expected. In the following, we will discuss the experimental results in more detail.

First, the formation of silver nanoparticles can be excluded for two reasons: The spectra cannot be reproduced by a linear combination of the spectra of gold and silver nanoparticles of the generated size. Second, at the chosen initial coverage the number density of gold nanoparticles is saturated and, therefore, all nucleation sites are occupied by nanoparticles. Assuming that the diffusion length of the silver atoms is similar to that of gold atoms, the deposited silver atoms can only bind to the already existing gold particles. Therefore, nanoparticles with a core-shell like structure or alloyed nanoparticles are formed.

In general, the increasing silver fraction leads to a change of the dielectric function and a homogeneous blue-shift of the plasmon resonance is expected [14], but not observed experimentally. This could be explained by a decreasing axial ratio of the nanoparticles, due to the growth process which leads to a competitive red-shift. But to explain the stable position of the surface plasmon resonance we have to assume a significant decrease of the axial ratio, which is very unlikely for Au/Ag-alloy nanoparticles. Therefore, production of Au/Ag-alloy nanoparticles by diffusion of the silver atoms into the gold nanoparticles can be excluded.

In contrast, the experimental data can be well explained by core-shell like nanoparticles. In fact, we do not expect, that the Ag-shell totally surrounds the Au-core, including the interface between the Au and the substrate. It is more realistic, to assume that the Ag-shell grows only on the gold-vacuum interface. Nevertheless, the non-complete shell has, if at all, only a minor effect, because only the (1,1)-mode has been investigated here. This mode corresponds to the electron excitation along the long axis of the nanoparticle parallel to the sample surface, where the Ag-shell surrounds the Au-core completely. Thus, for the modelling of the optical spectra we can assume a complete shell.

Depicted in Figure 3 are the modelled extinction spectra for pure gold and different core-shell nanoparticles with increasing fractions of silver, i.e. increasing silver shell thicknesses, with axial ratios and compositions as

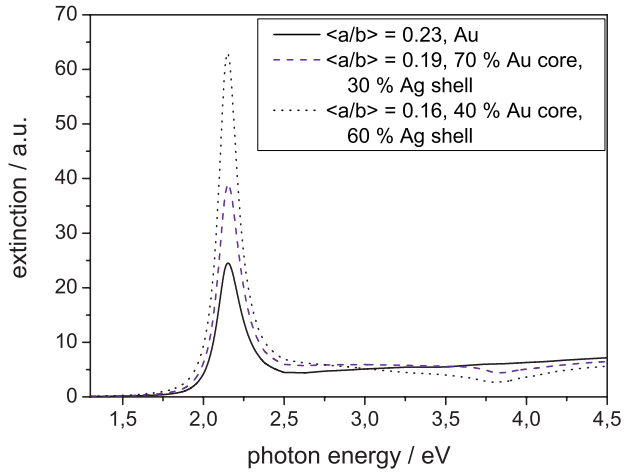

Fig. 3. Modelled extinction spectra of pure gold and Au-core/Ag-shell nanoparticles with increasing fractions of silver, i.e. increasing shell thickness. The composition of 40% Au and 60% Ag is the same as for core-shell nanoparticles with a Ag coverage of 2.08×10^{16} atoms/cm^2.

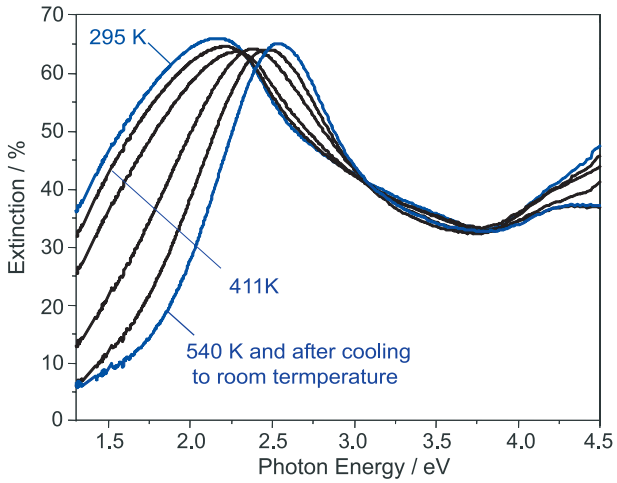

Fig. 4. Extinction spectra at different heating temperatures and after cooling down to room temperature after the final annealing at 540 K. For comparison, the as prepared spectrum of the core-shell nanoparticles is also depicted (295 K).

given in the inset. The surface plasmon resonance frequency remains constant with increasing silver shell thickness because the axial ratio decreases during growth. Furthermore, we do not see two distinct plasmon peaks as expected [14], since the gold peak is eventually damped by the silver shell, as also observed in reference [15]. Even though Au-core/Ag-shell nanoparticles are created in our experiments, we only see the Ag-shell plasmon resonance, which is nearly at the same position as the gold plasmon resonance for this particular axial ratio.

As a result, we can stabilize the plasmon resonance frequency independent of the silver coverage, i.e. the size of the nanoparticles. This cannot be achieved if pure gold or pure silver nanoparticles are made [16,17], unless laser assisted growth as shown in [18,19] is used.

In a second step the core-shell nanoparticles were annealed at elevated temperatures. Figure 4 shows the extinction spectra of the freshly prepared core-shell nanoparticles and for different annealing temperatures starting at 411 K and ending up at 540 K. The figure shows a clear shift of the surface plasmon resonance frequency with increasing temperature from 2.2 eV (λ = 564 nm) to 2.6 eV (λ = 477 nm), but almost no change of the extinction. If the annealed samples are cooled to room temperature, no additional changes of the spectrum are observed. The shift of the plasmon resonance is caused by two temperature dependent effects. First, alloying takes place [20] and nanoparticles with a composition of 40% gold and 60% silver are created, whose plasmon resonance is located between those of the two pure metals [21,22]. Second, a change of the shape towards spherical nanoparticles due to self-diffusion of atoms on the particle surface takes place [23]. The mean equivalent radius of the alloy nanoparticles was determined by scanning force microscopy to be $\langle R_{eq} \rangle = (12 \pm 1)$ nm.

To verify that alloy nanoparticle were produced, we have modelled the extinction spectra of Au/Ag-alloy nanoparticles with a material composition close to the composition of our nanoparticles. For this purpose one has to take into account that the dielectric function of the alloy is not necessarily a linear combination of the dielectric functions of the pure metals [21]. Hence, we have used modified dielectric functions taken from Ripken [24] and Schlüter [25], who investigated a thin alloy film containing 38% gold. The real part ϵ_1 in the range of 2.6 eV to 4.5 eV was taken from [24]. For the low energetic range the decrease of ϵ_1 predicted by the Drude-Lorentz theory for the free electron gas was fitted to the function. The imaginary part ϵ_2 in the range of 3.0 eV to 4.5 eV was also taken from [24]. In the lower energetic range ϵ_2 of the alloy can be approximated by the average of the values of the two components [25]. Thus, the dielectric functions of pure silver [26] and pure gold [27] were used to calculate ϵ_2 for photon energies lower than 3.0 eV. With this dielectric function the optical spectra of alloy nanoparticles were calculated.

The result of the modelling for single alloy nanoparticles together with a comparison to the experimental data is depicted in Figure 5. Since the axial ratio of the nanoparticles is unknown, we have used a value of $\langle a/b \rangle = 0.33$, which best fits to our experimental results. Although there is a small difference in the composition, the energetic position of the resonance is the same for the experimental and the modelled data within the experimental errors. The width of the measured extinction spectrum is broader than the computed one due to the size and shape distributions of the nanoparticles, which cause inhomogeneous broadening.

4 Conclusion

In our experiments we have deposited silver atoms on gold nanoparticles to prepare core-shell structures. It has been shown, that we can stabilize the plasmon resonance of the

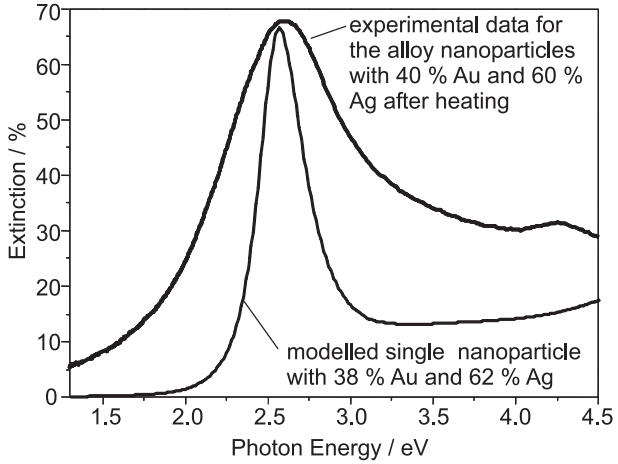

Fig. 5. Extinction spectra of annealed Au-core/Ag-shell nanoparticles and the modelled spectra for alloy nanoparticles with a composition of 38% Au and 62% Ag and an axial ratio of 0.33.

nanoparticles at a certain energy of approximately 2.2 eV, even though the silver shell growths and the overall size of the nanoparticle increases. Such stabilization is impossible for pure silver or gold nanoparticles. Furthermore, by annealing the nanoparticles we can tune the surface plasmon frequency from 2.2 eV to 2.6 eV. The shift is caused by a change in shape towards spherical nanoparticles and by alloying of the core-shell particles.

With this method we can produce small nanoparticles with *tunable* plasmon resonance frequencies in order to optimize the absorption wavelength, the amplitude and the enhancement factor independently.

Further experiments are in progress with Au-core/Ag-shell as well as with Ag-core/Au-shell nanoparticles to improve the tuning even further. In addition, experiments with *p*-polarized light will also make it possible to measure the (1,0)-mode.

Financial support by the European Union under contract HPRN-CT-2002-00328 NanoCluster is gratefully acknowledged. This work was also founded in part by the Fonds der Chemischen Industrie and the Kasseler Hochschulbund. F.H. is also grateful to the German Science Foundation.

References

1. K. Kneipp, Y. Wang, H. Kneipp, L.T. Perelman, I. Itzkan, R.R. Dasari, M.S. Feld, Phys. Rev. Lett. **78**, 1667 (1997)
2. S. Nie, S.R. Emory, Science **275**, 1102 (1997)
3. G. Chumanov, T.M. Cotton, Proc. SPIE **3608**, 204 (1999)
4. I. Gryczynski, J. Malicka, Y. Shen, Z. Gryczynski, J. Lakowicz, J. Phys. Chem. **106**, 2191 (2002)
5. J. Lakowicz, B. Shen, Z. Gryczynski, S. D'Auria, I. Gryczynski, Biochem. Biophys. Res. Com. **286**, 875 (2001)
6. J. Lakowicz, Analyt. Biochem. **298**, 1 (2001)
7. M. Alschinger, M. Maniak, F. Stietz, T. Vartanyan, F. Träger, Appl. Phys. B **76**, 771 (2003)
8. J.R.F. Haglund, L. Yang, R.M. III, J.E. Wittig, K. Becker, R.A. Zuhr, Opt. Lett. **18**, 373 (1993)
9. J. Krenn, H. Ditlbacher, G. Schider, A. Hohenau, A. Leitner, F.R. Aussenegg, J. Microscopy **209**, 167 (2003)
10. J. Krenn, Nature Mat. **2**, 210 (2003)
11. F. Stietz, J. Bosbach, T. Wenzel, T. Vartanyan, A. Goldmann, F. Träger, Phys. Rev. Lett. **84**, 5644 (2000)
12. J. Bosbach, D. Martin, F. Stietz, T. Wenzel, F. Träger, Appl. Phys. Lett. **74**, 2605 (1999)
13. U. Kreibig, M. Vollmer, *Optical properties of metal clusters* (Springer, Berlin, 1995)
14. J. Sinzig, U. Radke, M. Quinten, U. Kreibig, Z. Phys. D **26**, 224 (1993)
15. P. Mulvaney, M. Giersig, H. Henglein, J. Phys. Chem. **97**, 7061 (1993)
16. F. Hubenthal, T. Ziegler, C. Hendrich, T. Vartanyan, F. Träger, Proc. SPIE **5221**, 29 (2003)
17. T. Wenzel, J. Bosbach, A. Goldmann, F. Stietz, F. Träger, Appl. Phys. B **69**, 513 (1999)
18. F. Stietz, Appl. Phys. A **72**, 381 (2001)
19. F. Hubenthal, C. Hendrich, H. Ouacha, D. Blázquez Sánchez, F. Träger, Int. J. Mod. Phys. B (accepted, 2005)
20. J.H. Hodak, A. Henglein, G.V. Hartland, J. Phys. Chem. B **104**, 9954 (2000)
21. S. Link, Z.L. Wang, M.A. El-Sayed, J. Phys. Chem. B **103**, 3529 (1999)
22. M. Moskovits, I. Srnová-Sloufová, B. Vlcková, J. Chem. Phys. **116**, 10435 (2002)
23. M. Drechsler, Surf. Sci. **108**, 549 (1981)
24. K. Ripken, Z. Phys. **250**, 228 (1972)
25. M. Schlüter, Z. Phys. **250**, 78 (1972)
26. D. Edward, I. Palik, *Handbook of optical constants of solids* (Academic Press, Orlando, Florida, 1985)
27. P.B. Johnson, R.W. Christy, Phys. Rev. B **6**, 4370 (1972)